Title

Cell-secreted matrices perpetuate the bone-forming phenotype of differentiated mesenchymal stem cells

Authors

Hoch, Allison I
Mittal, Vaishali
Mitra, Debika
et al.

Publication Date

2016

DOI

10.1016/j.biomaterials.2015.10.003

Peer reviewed

HHS Public Access

Author manuscript

Biomaterials. Author manuscript; available in PMC 2017 January 01.

Published in final edited form as:

Biomaterials. 2016 January ; 74: 178–187. doi:10.1016/j.biomaterials.2015.10.003.

Cell-secreted matrices perpetuate the bone-forming phenotype of differentiated mesenchymal stem cells

Allison I. Hoch[a], **Vaishali Mittal**[a], **Debika Mitra**[a], **Nina Vollmer**[a], **Christopher A. Zikry**[a], and **J. Kent Leach**[a,b,*]

[a]Department of Biomedical Engineering, University of California, Davis, Davis, CA 95616

[b]Department of Orthopaedic Surgery, School of Medicine, University of California, Davis Sacramento, CA 95817

Abstract

Prior to transplantation, mesenchymal stem/stromal cells (MSCs) can be induced toward the osteoblastic phenotype using a cocktail of soluble supplements. However, there is little evidence of differentiated MSCs directly participating in bone formation, suggesting that MSCs may either die or revert in phenotype upon transplantation. Cell-secreted decellularized extracellular matrices (DMs) are a promising platform to confer bioactivity and direct cell fate through the presentation of a complex and physiologically relevant milieu. Therefore, we examined the capacity of biomimetic DMs to preserve the mineral-producing phenotype upon withdrawal of the induction stimulus. Regardless of induction duration, ranging up to 6 weeks, MSCs exhibited up to a 5-fold reduction in osteogenic markers within 24 hours following stimulus withdrawal. We show that seeding osteogenically induced MSCs on DMs yields up to 2-fold more calcium deposition than tissue culture plastic, and this improvement is at least partially mediated by increasing actin cytoskeletal tension *via* the ROCK II pathway. MSCs on DMs also secreted 25% more vascular endothelial growth factor (VEGF), a crucial endogenous proangiogenic factor that is abrogated during MSC osteogenic differentiation. The deployment of DMs into a subcutaneous ectopic site enhanced the persistence of MSCs 5-fold, vessel density 3-fold, and bone formation 2-fold more than MSCs delivered without DMs. These results underscore the need for deploying MSCs using

Address for correspondence: J. Kent Leach, Ph.D., Department of Biomedical Engineering, University of California, Davis, 451 Health Sciences Drive, Davis, CA 95616, (530) 754-9149 (phone), (530) 754-5739 (fax), jkleach@ucdavis.edu.

Allison I. Hoch: Conception and design, financial support, collection and/or assembly of data, data analysis and interpretation, manuscript writing
Vaishali Mittal: Collection and/or assembly of data
Debika Mitra: Collection and/or assembly of data
Nina Vollmer: Collection and/or assembly of data
Christopher A. Zikry: Collection and/or assembly of data
J. Kent Leach: Conception and design, financial support, data analysis and interpretation, manuscript writing, final approval of manuscript

DISCLOSURE OF POTENTIAL CONFLICTS OF INTEREST
The authors indicate no potential conflicts of interest.

biomaterial platforms such as DMs to preserve the *in vitro*-acquired mineral-producing phenotype and accelerate the process of bone repair.

Keywords

Mesenchymal stem/stromal cells; extracellular matrix; osteogenesis; dedifferentiation; bone

INTRODUCTION

Mesenchymal stem/stromal cells (MSCs) are a promising cell population in therapies for bone repair due to their proliferation, osteogenic potential, and secretion of potent endogenous trophic factors to enhance local vascularization. MSCs commonly undergo biochemical induction in culture to direct them towards the osteoblastic phenotype, yet the ideal duration of osteoinduction remains unknown [1–3]. The lack of evidence demonstrating the successful incorporation of transplanted MSCs into repair bone suggests either not enough cells were used [4] or cells may undergo a number of potential fates: the duration of osteogenic induction may be insufficient to lock MSCs into the osteoblastic lineage, MSCs may undergo apoptosis and/or fail to engraft in the defect site, and MSCs may participate in bone formation indirectly through the secretion of potent proangiogenic factors such as vascular endothelial growth factor (VEGF) [5]. Extended induction periods in monolayer culture compromise MSC progenitor potency [6–10], significantly impair VEGF secretion [11, 12], suffer from increased risk for contamination, and are not clinically relevant [10].

MSCs are commonly induced toward the osteoblastic lineage by culturing cells in a soluble cocktail of ascorbic acid (AA), β-glycerophosphate (βGP), and dexamethasone (DEX) [13]. It remains unknown whether the aforementioned biochemical cocktail is sufficient to lock MSCs into an osteogenic phenotype, and if so, how long MSCs must be maintained in this environment. Following a 4 week induction period, MSC osteogenic gene expression decreased upon stimulus withdrawal. Furthermore, osteogenically induced MSCs retained adipogenic potential [14]. These data suggest MSCs induced solely using soluble cues from an osteogenic cocktail do not cement MSCs into a permanent osteoblastic phenotype.

The extracellular matrix (ECM) presents glycoprotein motifs that support cellular adhesion and juxtapose molecular cues in the form of chemokines and growth factors that guide cell adhesion, migration, and tissue formation. Tissue engineering approaches seek to incorporate the biomimetic characteristics of ECM, either by coating material surfaces with recombinant ECM proteins and peptides [15] or by employing decellularized allogeneic or xenogeneic tissue as scaffolding [16]. However, the former strategy fails to capture the complex composition and architecture characteristic of native ECM, and the latter suffers from immunological, reproducibility, and availability concerns. Recently, we established the translation of novel cell-secreted decellularized extracellular matrices (DMs), which retain osteogenic and proangiogenic potency when stored on the shelf and when transferred to scaffolds [17–19].

Given the uncertainty over whether differentiated or undifferentiated MSCs facilitate more bone *in vivo* [1–3], we hypothesized: 1) increasing the duration of osteoinduction up to 6 weeks using the common cocktail does not cement the osteoblastic phenotype, and 2) DMs would better preserve the mineral-producing phenotype of MSCs established by the common osteogenic cocktail. To test this hypothesis, we cultured MSCs in osteogenic media for up to 6 weeks and measured the regression of osteogenic markers upon withdrawal of the induction cocktail. Subsequently, osteogenically induced MSCs were seeded onto DMs and analyzed for osteogenic and proangiogenic markers upon the withdrawal of the induction cocktail. The ability of osteogenically induced MSCs delivered with and without DMs to promote vascularization and produce bone was evaluated using alginate hydrogels in an ectopic tissue site, simulating the absence of potent osteogenic cues. The results of these studies highlight the rationale for delivering MSCs with DMs in order to sustain the mineral-producing phenotype and the secretion of proangiogenic trophic factors, thereby increasing the efficacy of MSCs in cell therapies for bone repair.

MATERIALS AND METHODS

Cell culture

Human bone marrow-derived MSCs (Lonza) were expanded without further characterization and passaged prior to confluency in growth medium: alpha-modified minimum essential media (α-MEM, Invitrogen) supplemented with 10% fetal bovine serum (FBS, JR Scientific) and 1% penicillin (10,000 U/mL) and streptomycin (10 mg/mL) (P/S, Gemini). MSCs were derived from three male donors ranging from 20–30 years old and expanded under standard culture conditions. Osteogenic media consisted of growth media supplemented with 50 μg/mL ascorbate-2-phosphate (A2P), 10 mM β-glycerophosphate (βGP), and 10 nM dexamethasone (DEX) (all from Sigma) [11]. Media changes were performed every third day.

Osteogenic induction and withdrawal procedure

MSCs were seeded at 2,000 cells/cm^2 in 225 cm^2 flasks (Corning) and cultured for 2 weeks prior to passage. MSCs were trypsinized and seeded at 30,000 cells/cm^2 in 12-well plates (BD Falcon) for the last 2 weeks before stimulus withdrawal, including the entirety of the 2-week study. MSCs were passage 5 at the time of analysis for every group. MSCs were cultured in growth media or osteogenic media for 2, 4, or 6 weeks. To extract cells after 2 week culture periods, MSCs were incubated with 0.3% collagenase II (Worthington 4176) for 5 minutes prior to adding 0.05% trypsin/0.53 mM EDTA (Corning).

Osteogenic and proangiogenic potential

Intracellular alkaline phosphatase (ALP) activity was quantified as previously described [11] and normalized to total DNA content from the same cell lysate as quantified using Quant-iT PicoGreen dsDNA Assay Kit (Invitrogen). Calcium deposition was quantified as previously described [20] and was normalized to total DNA. Calcium deposition was visualized using 2% Alizarin Red S (Sigma) solution after fixation in 4% formalin. Gene expression was assessed by quantitative PCR as previously described [11]. Primers and probes consisted of *IBSP* (bone sialoprotein, Hs00173720_m1) and *RPL13* (ribosomal protein L13,

Hs00204173_m1) (Applied Biosystems). Quantitative PCR results were normalized to housekeeping transcript level (*RPL13*) to yield ΔCt. Fold changes between GM were calculated to yield ΔΔCt. Data are presented as $2^{-\Delta\Delta Ct}$ and standard deviation was calculated according to the manufacturer's protocol.

The concentration of VEGF in 1 mL of MSC conditioned media over 24 hours was determined using a human VEGF ELISA kit (R&D Systems) as previously described [11] and normalized to DNA content from the same well.

Morphology and colony-forming efficiency (CFE)

MSC morphology was qualitatively and quantitatively assessed after 2, 4, or 6 weeks of culture in growth or osteogenic media following a final passage seeded at 2,000 cells/cm^2. The number of spindle-shaped cells was counted using 10× bright field microscopy for 20 fields of view. Average cell length was calculated *via* NIH ImageJ for approximately ten cells per five fields of view using 10× bright field microscopy.

To assess colony-forming efficiency (CFE), 300 MSCs were plated in a ≈59cm^2 circular tissue culture dish (BD Falcon) and cultured for 2 weeks in growth media regardless of previous conditioning. After 2 weeks, colonies were fixed in 4% formalin, stained with crystal violet solution (Sigma), and counted [7, 8]. CFE for each group was normalized to that of MSCs in growth media for 2 weeks within each of three donors.

Adipogenic potential as an indicator of MSC plasticity

After culture in growth media or osteogenic media, MSCs were reseeded at 30,000 cells/cm^2 in 12-well plates and cultured in osteogenic media or alternating induction and maintenance adipogenic medium (Lonza PT-3004) for 3 weeks to induce osteogenic and adipogenic differentiation, respectively. Osteogenesis was visualized as described above. Adipogenesis was visualized by applying a 0.4% Oil Red O (Sigma) solution to MSCs after fixation in 60% isopropanol.

Preparation and characterization of cell-secreted decellularized extracellular matrices (DMs)

DMs were prepared as previously described [17, 18, 20]. Briefly, MSCs were seeded at 50,000 cells/cm^2 and cultured in supplemented media (SM: α–MEM containing 10% FBS, 1% P/S, and 50 μg/mL ascorbate-2-phosphate). Plates were decellularized using a series of washes containing PBS, 0.5% Triton X-100, 20 mM NH_4OH, and 200 U/mL DNAse. DMs were dried aseptically in a biosafety cabinet for up to 12 hours, and stored at room temperature in the dark for up to 1 month prior to use. DMs from 5 wells were pooled per sample (n = 3) and collected in 0.02 N acetic acid (50 μL per well in a 6-well plate), transferred to a microcentrifuge tube and sonicated on ice 10–15 times with 5 second pulses at 40% amplitude to mechanically homogenize the DM contents. Protein concentration was determined using a bicinchoninic acid (BCA) assay (Thermo Fisher Scientific). Protein was qualitatively visualized using a 0.2% Coomassie Brilliant Blue solution dissolved in 20% methanol, 0.05% acetic acid, and 79.5% water for 15 minutes. In agreement with our previous studies [19, 20], DMs lacked mineralization, ALP activity, and bound VEGF.

MSC response to cell-secreted decellularized extracellular matrices (DMs)

MSCs were induced in osteogenic media for 2 weeks prior to seeding on DM because extended durations did not preserve the mineral-producing phenotype and are not clinically relevant. Assessment of calcium deposition, VEGF secretion, intracellular ALP activity, and DNA content were performed as described above. MSCs were exposed to Y-27632 dihydrochloride (10 μM, Tocris Bioscience) for 24 hours to inhibit actin tension via ROCK II. Cytoskeletal tension was visualized with F-actin staining using rhodamine phalloidin (0.165 μM, Life Technologies). Nuclei were visualized by counterstaining with SYTOX® Green (1 μM, Life Technologies).

To evaluate MSC response to a single extracellular matrix constituent, wells were coated with human fibronectin (h FN, 5 $\mu g/cm^2$, R&D), human collagen type I (h Col I (1×: 5 $\mu g/cm^2$ or 2×: 10 $\mu g/cm^2$, R&D), rat tail collagen type I (r Col I, 5 $\mu g/cm^2$, BD Biosciences), or human laminin-α4 (h Laminin, 5 $\mu g/cm^2$, R&D).

Preparation of alginate hydrogels containing DM-coated microcarrier beads

To evaluate the persistence of implanted cells in the ectopic site, *in vivo* studies utilized luciferase-transduced MSCs (Luc-MSCs). Four groups were prepared using irradiated alginate hydrogels as a delivery vehicle: Luc-MSCs cultured 2 weeks in growth media (GM), Luc-MSCs cultured 2 weeks in osteogenic media (OM), Luc-MSCs cultured 2 weeks in growth media and seeded on DM-coated microcarrier beads (GM-DM), Luc-MSCs cultured 2 weeks in osteogenic media and seeded on DM-coated microcarrier beads (OM-DM).

To produce 10 gels, 15 mg of Cytodex® 3 microcarrier beads (~175 μm, GE Healthcare) were swelled in PBS for 3 hours, sterilized in 70% ethanol overnight, and rinsed with PBS [19]. 15 mg of beads and 100 μL of DM solution (2250 μg/mL in 0.02 N acetic acid) were added to silanized (Sigmacote, Sigma) wells of a 48-well plate and allowed to dry overnight [19]. 1 mL (20 million cells per mL) of 2 week conditioned GM or OM Luc-MSCs were added to a FACs tube containing either 500 μL DM-bead solution in α-MEM (GM-DM and OM-DM) or 500 μL α-MEM (GM and OM) and shaken every 30 minutes for 4 hours to coat the DM-beads with cells. After 4 hours, the supernatant was removed and 800 μL of irradiated 2.5% (w/v) alginate (Pronova UP MVG, Novamatrix) was added to 200 μL of the Luc-MSC-coated DM-beads to achieve a final concentration of 2.0% (w/v) alginate. 100 μL of this alginate solution was pipetted into cylindrical silicon molds (8 mm × 1.5 mm) with an extra 20 μL dome and polymerized with 200 mM calcium chloride solution through dialysis paper for 10 minutes at room temperature. Subsequently, all gels were cultured in 1 mL GM on an XYZ-shaker for 24 hours before implantation. The number of adherent cells was measured using a DNA assay to confirm similar numbers of MSCs were deployed in each experimental group.

Rheology of MSC-loaded alginate hydrogels

The shear storage moduli of MSC-containing (20 million cells per mL) hydrogels in the presence or absence of DM-coated beads was evaluated using a Discovery HR2 Hybrid Rheometer (TA Instruments). Gels were maintained in media under standard culture

conditions for 24 hours before rheology measurements to mimic the same culture duration before implantation. An oscillatory sweep of 0.004–4% strain was performed on each hydrogel using an 8.0 mm diameter Peltier Plate geometry. Storage moduli in the linear viscoelastic region were averaged and resultant averages were calculated from $n \geq 6$ gels.

Murine subcutaneous implant model

Treatment of experimental animals was in accordance with the UC Davis animal care guidelines and all National Institutes of Health animal-handling procedures. Eight-week-old non-obese diabetic/severe combined immunodeficient gamma (NSG, NOD.Cg-Prkdc^{scid} Il2rg^{tm1Wjl}/SzJ) mice (Jackson Laboratories) were anesthetized and maintained under a 2% isoflurane/O_2 mixture delivered through a nose cone. Every animal received four subcutaneous implants containing GM (upper left), OM (upper right), GM-DM (lower left), and OM-DM (lower right).

Cell persistence was measured using *in vivo* whole body bioluminescence at 0, 4, 7, 14, and 21 days on an IVIS Spectrum (Perkin Elmer) as described [21]. Total photons per second per square centimeter were recorded from each bioluminescent region of interest. Animals were euthanized 2 weeks ($n = 6$) and 8 weeks ($n = 6$) post-surgery. Each gel was excised and fixed in 10% formalin and then processed for histology using standard techniques. Vessel density at 2 weeks was quantified using H&E stained cross-sections and consisted of counting circular structures with well-defined lumens containing more than one erythrocyte. Total bone volume at 8 weeks was visualized and quantified using microcomputed tomography (μCT) [21]. The hydrogel was imaged (45 kVp, 177 μA, 400 μs integration time, average of four images) using a high-resolution μCT specimen scanner (μCT 35; Scanco Medical). Approximately 696 contiguous slices of 2048×2048 pixels were imaged with 6 μm resolution and slice thickness (voxels). Serial tomograms were reconstructed from raw data of 1000 projections per 180° using an adapted cone beam-filtered back projection algorithm [22]. The tomograms were calibrated to a range of concentrations of HA 0.0, 99.6, 200.0, 401.0, and 800.3 mg HA/cc in order to convert grey-values (x-ray attenuation) of the images to units of density in mg HA/cc. A threshold (282–3000 mg HA/cc) was determined subjectively from the reconstructed images to partition mineralized tissue from fluid and soft-tissues. After thresholding, the image noise was reduced using a low-pass Gaussian filter (σ=0.8, support=1). A circular region of 0.83 cm^2 was centered on the hydrogel cross-section to create a cylindrical volume. The length of the cylinder was created large enough to surround each individual scaffold based on its size.

Statistical analysis

Data from *in vitro* studies are presented as means ± standard deviation from at least three independent experiments with 3–4 technical replicates per donor. Trends in multilineage potential, morphology, CFE, 6 week ALP and calcium, and +5d calcium employing DMs were confirmed using MSCs from three donors. For three groups within a time point, statistical significance was assessed by one-way ANOVA followed by a Newman–Keuls *post hoc* test and p-values < 0.05 were considered statistically significant. For two groups within a time point, statistical significance was assessed by an unpaired two-tailed t-test and p-values < 0.05 were considered statistically significant. A minimum of four animals per

time point was analyzed to assure a p-value < 0.05 and a power of 80% with an assumed standard deviation of 10%. MicroCT collection and analysis were blinded. Statistical analysis was performed using GraphPad Prism® 4 analysis software.

RESULTS

Differentiated MSCs exhibit a rapid regression of osteoblastic markers upon stimulus removal

Fig. 1A illustrates the procedure for osteogenic induction and stimulus withdrawal. Specifically, MSCs were cultured in growth media or osteogenic media for 2, 4, or 6 weeks. After each culture period, the osteogenic cocktail was replaced with growth media for an additional 5 days (OM/GM). As a positive control, osteogenically induced MSCs remained in osteogenic media (OM). MSCs cultured in growth media for the full duration (GM) served as the negative control. Osteogenic markers were assessed at 0d (baseline), +1d, and +5d where 0d marks the day media was switched. MSCs were cultured for 2, 4, or 6 weeks in growth media or osteogenic media and stained with Alizarin Red S to visualize mineralization at 0d (Fig. 1B). GM displayed no appreciable staining across all time points, whereas OM/GM and OM displayed comparable positive staining that increased with increasing duration.

Regardless of induction duration, OM/GM exhibited significantly lower ALP activity +1d after cocktail removal (Fig. 1D) compared to OM. We observed a consistent trend in ALP activity regression across three donors. By +5d, OM/GM exhibited ALP activity comparable to or less than GM. Similar to ALP activity, MSCs deposited less calcium +1d after stimulus removal following 2, 4, or 6 weeks of osteogenic differentiation (Fig. 1E). Like ALP activity, the trend in calcium deposition regression extended across three donors. Bone sialoprotein (*IBSP)* gene expression is a late marker sustained at high levels throughout long-term osteogenic induction [23]. We examined the regression of *IBSP* after 4 weeks of differentiation to reflect the timeline of previous studies [14]. Stimulus withdrawal from 4 week-induced MSCs diminished *IBSP* expression 4-fold in 24 hours to levels statistically similar to MSCs maintained in growth media (GM) (Fig. 1C), thereby demonstrating the implications of stimulus withdrawal extend to a transcriptional level.

Differentiated MSCs exhibit osteoblastic characteristics yet retain adipogenic potential

The transition from a fibroblastic to cuboidal-shaped morphology in MSCs has been used to identify an osteoblastic phenotype [23, 24]. After 2 weeks in culture, GM exhibited distinct spindle-shaped morphology, while OM developed a cuboidal morphology with an enlarged nucleus (Fig. S1A–C). We investigated colony-forming efficiency (CFE) because it has been correlated with remaining cumulative population doublings [25], multilineage potential [26], and subsequent bone formation [27]. Osteogenically differentiated MSCs exhibited a greater CFE than MSCs cultured in growth media (Fig. S1D–E). However, regardless of osteogenic differentiation and withdrawal protocol (Fig. S2A), MSCs retained the ability to differentiate toward both the osteogenic and adipogenic lineages. MSCs from all differentiation protocols stained positively and similarly for Alizarin Red S and Oil Red O, respectively (Fig. S2B). MSCs osteogenically induced (OM/GM and OM) for 6 weeks and after each stimulus

withdrawal period exhibited areas where cells deposited mineral while simultaneously producing oil droplets during adipogenic differentiation (Fig. S2B).

Proliferation and VEGF secretion are impaired during osteogenic differentiation

We measured DNA content to probe MSC proliferation. GM exhibited higher DNA content than OM at all time points (Fig. 2A), reflective of the well-known shift from proliferation to commitment during MSC induction. VEGF secretion was greatest for GM compared to OM after 2 and 4 weeks (Fig. 2B). After 6 weeks, GM consistently secreted the least VEGF, and OM/GM secreted the greatest concentration of VEGF after +5d of stimulus withdrawal. For all induction periods, OM/GM secreted more VEGF compared to OM after +5d, suggesting that VEGF secretion may be an indicator of MSC osteodifferentiation state in this model [11].

DMs simultaneously promote the osteogenic and proangiogenic potential of differentiated MSCs in the absence of soluble osteoinductive cues

Using MSCs differentiated for 2 weeks in an osteogenic cocktail, we investigated whether cell-secreted decellularized matrices (DMs) could sustain the mineral-producing phenotype in the absence of soluble osteoinductive cues. We selected an induction period of two weeks because prolonged durations up to 6 weeks did not preserve commitment, and lengthy culture durations are not clinically relevant. DMs were prepared as previously described [20] (Fig. 3A). DMs lacked cells and cell-secreted mineral, yet were rich in protein when qualitatively observed (Fig. S3A) and quantified (7.02 ± 0.44 μg protein/cm^2, $n = 3$). In the absence of the osteogenic cocktail, osteogenically differentiated MSCs seeded on DMs ((+) DM) deposited significantly more normalized calcium than cells on tissue culture plastic ((−) DM) (Fig. 3B). We confirmed the trend at +5d in normalized calcium using MSCs from three donors (Fig. 3C). MSCs proliferated slightly less when seeded on DMs (Fig. S3B), yet the average total calcium deposition of osteogenically differentiated MSCs from three donors seeded on (+) DM was greater than those seeded on (−) DM at +5d (Fig. 3E). Thus, DNA content did not significantly skew the implication from the normalized calcium results. Despite significant increases in calcium deposition, we did not observe appreciable differences in ALP activity between culture platforms (Fig. S3C). Importantly, MSCs seeded on (+) DM generally secreted more VEGF than cells seeded on (−) DM at both +1d and +5d (Fig. 3D).

We seeded osteogenically induced MSCs on other extracellular matrix proteins to investigate whether an individual matrix component would elicit a similar sustained osteogenic response as (+) DM. The individual matrix proteins were selected based on data from our group and others reporting their roles in osteogenesis and cell adhesion [17, 28–30]. At both +1d and +5d, MSCs seeded on (+) DM exhibited significantly more normalized calcium than cells on (−) DM or any of the alternative matrices: human fibronectin (h FN), human collagen type I (h Col I (1×), rat tail collagen type I (r Col I), human laminin-α4 (h Laminin) (Fig. 4A). The total calcium deposition by MSCs seeded on (+) DM was greater than those seeded on (−) DM and other matrix proteins at +5d (Fig. S4A). We observed similar trends in VEGF secretion by MSCs on each matrix at +5d. MSCs seeded on (+) DM secreted more VEGF compared to cells on (−) DM and other matrix proteins (Fig. S4B).

F-actin staining revealed that MSCs were more elongated on (+) DM than (−) DM (Fig. 4B). Increased cell spreading can regulate MSC commitment toward the osteogenic lineage, specifically *via* RhoA, a protein that adjusts the actin cytoskeleton through the formation of stress fibers, and its effector ROCK [31]. Treatment with Y-27632 (10 μM) demonstrated that osteogenically differentiated MSCs seeded on (+) DM were more susceptible to inhibition of ROCK II (Rho kinase II), illustrated by thinner cell morphology compared to MSCs on (−) DM. Furthermore, *IBSP* expression of osteogenically differentiated MSCs seeded on (+) DM was abrogated in the presence of Y-27632, whereas expression by those seeded on (−) DM remained unchanged (Fig. 4C). Thus, DMs function by preserving the osteogenic phenotype of MSCs at least partially by increasing cytoskeletal tension.

DMs enhance MSC persistence, vessel density, and bone formation in an ectopic site

Luciferase-transduced MSCs were delivered as dissociated cells or seeded directly on DM-coated Cytodex® microbeads and suspended in alginate gels (Fig. 5A) for deployment to an ectopic site. Approximately 82% of the initially-loaded MSCs adhered to the beads in all formulations, regardless of the presence of DM or induction protocol. The addition of DM-coated beads to alginate gels did not significantly impact the storage modulus of cell-seeded gels when measured using rheology (Fig. 5B). Osteogenically differentiated MSCs seeded on DMs persisted better than other groups up to 3 weeks post implantation (Fig. 5C) and yielded nearly 3-fold greater blood vessel density of explants at 2 weeks (Fig. 5D). At 8 weeks, osteogenically differentiated MSCs seeded on DMs significantly enhanced bone formation compared to dissociated induced MSCs or undifferentiated MSCs delivered with or without DMs (Fig. 5E). While most groups exhibited mineralization on the perimeter of the hydrogel, only gels containing osteogenically differentiated MSCs seeded on DMs exhibited significant mineralization in the center as well.

DISCUSSION

Cell-based therapies for tissue defects are predicated on the assumption that the transplantation of a specific cell population can directly form replacement tissues, thereby accelerating replacement of lost tissue volume. MSCs are commonly differentiated toward the osteoblastic lineage by culturing in a cocktail of supplements. It is commonly assumed that the resulting changes in phenotype are preserved after removal of the stimulus, yet MSC commitment has not been conclusively established. Indeed, it is still unclear whether induced MSCs have greater therapeutic potential in bone formation than undifferentiated MSCs *in vivo* [1–3]. Compared to MSCs cultured continuously in the osteogenic cocktail, these data reveal that MSCs exhibited significant decreases in early and late osteogenic markers as early as 24 hours after withdrawal of the cocktail. Importantly, after 5 days of induction withdrawal, MSCs previously differentiated for 2 weeks regressed in calcium deposition to a level similar to undifferentiated MSCs. MSCs differentiated for clinically relevant induction periods (*e.g.*, 2–4 weeks) exhibited reduced VEGF secretion, representing a significant limitation due to the role of angiogenesis in bone repair [21, 32–34]. In light of these limitations of the osteogenic cocktail, we employed cell-secreted decellularized extracellular matrices (DMs) as a novel approach to direct cell fate through the presentation of a complex and physiologically relevant milieu. In the present study, we demonstrate that

DMs uniquely enhanced both calcium deposition and VEGF secretion of differentiated MSCs subsequently removed from exposure to the osteogenic cocktail.

The concept of plasticity postulates that lineage determination of a differentiating stem cell is malleable [35]. MSCs osteogenically induced for 3 weeks produced both oil and sulfated proteoglycans upon subsequent adipogenic and chondrogenic differentiation, respectively [14]. In our study, we doubled the differentiation window from 3 to 6 weeks and demonstrated extensive mineral-depositing MSCs could still be induced to produce oil. The retention of adipogenic potential, despite long-term osteogenic induction, is striking because many speculate osteogenesis is the default pathway for MSCs [9]. Cuboidal-shaped MSCs reflect a characteristic osteoblast phenotype [23, 24] that has been correlated to an erosion of progenitor properties such as proliferation rate [6, 36, 37]. We observed a significant fraction of cuboidal-shaped MSCs following differentiation for 2 weeks, yet the same culture regressed in osteogenic markers and retained adipogenic potential. The transition from mineral deposition to oil production may have relevance to osteopenic disorders wherein skeletal integrity is compromised by the increase in adipocytes that occur at the expense of osteoblasts [38].

Once we established that MSCs remained plastic, even after 6 weeks of induction using the osteogenic cocktail, we sought to improve mineral production in the absence of soluble cues in order to address the significant clinical challenge of osteoinduced cells failing to directly contribute to bone formation. In addition to preserving calcium deposition, we demonstrate DMs preserve the secretion of VEGF, which confirms our previous data wherein DMs enhance transcriptional expression of *VEGF* [18, 19]. We and others have shown osteogenically induced MSCs secrete low levels of VEGF during early differentiation [11] and high levels of VEGF during late differentiation [12]. That DMs maintain both MSC osteogenic and proangiogenic potential is noteworthy because the latter is typically sacrificed in lieu of osteogenic differentiation [11], yet both are requisite for successful bone repair [21, 32–34].

We propose DMs preserve the mineral-producing phenotype at least partially by increased myosin-generated cytoskeletal tension. Such tension regulates MSC commitment toward the osteogenic lineage, specifically *via* modulation of RhoA, a small GTPase protein, and its effector ROCK [31]. Our data are in agreement with a previous study demonstrating that compliance of type I collagen-functionalized substrates regulated osteogenic differentiation through MAPK activation downstream of the RhoA-ROCK signaling pathway [29]. We have previously shown the MAPK/ERK pathway [20] to mediate the osteogenic differentiation of MSCs seeded on DMs.

In a subcutaneous tissue site, osteogenically induced MSCs seeded on DMs persisted better than undifferentiated MSCs seeded on DMs, which corroborates our previous findings that osteogenic priming may enhance persistence [39]. We employed alginate hydrogels as a delivery vehicle in part due to their inherent lack of osteoinductive cues. MSCs did not persist as effectively without DMs because the hydrophilic nature of alginate does not support protein adsorption and subsequent cellular attachment [40]. Moreover, we previously demonstrated that MSCs deployed in alginate gels with uncoated microbeads

exhibited reduced osteogenic differentiation and bone formation *in vivo* compared to DM-coated beads, providing additional evidence of this substrate's potency to instruct cell function [19]. The comparable storage moduli of alginate gels in the presence or absence of DM-coated beads suggests gel mechanical properties were likely not responsible for subsequent osteogenic response [41]. The subcutaneous mouse model lacks other stimuli present in large bone defects such as endogenous osteoinductive cues and potential mechanical loading, as well as increased vascularization. After 2 weeks, osteogenically induced MSCs seeded on DMs enhanced vascular density, data that are supported by improved persistence *in vivo* using osteogenically induced MSCs and in agreement with our *in vitro* findings that DMs augmented VEGF secretion. After 8 weeks, osteogenically induced MSCs seeded on DMs exhibited significantly more mineralization in a subcutaneous tissue site than other groups. These data demonstrate the necessity for providing continued instruction to MSCs upon transplantation to capitalize on the induced phenotype following biochemical induction. This study has relevance toward the treatment of bone defects in which MSCs have exhibited a poor history of survival and engraftment. Future studies will evaluate this platform in orthotopic bone defects to advance the clinical application of these findings.

Supplementary Material

Refer to Web version on PubMed Central for supplementary material.

ACKNOWLEDGMENTS

This study was supported in part by the National Institutes of Health (R03-DE021704) and the AO Foundation (C10-39L) to JKL. AIH is grateful for financial support through the ARCS Foundation, Inc., Northern California Chapter, and an industry/campus-supported fellowship under the NIH Training Program in Biomolecular Technology (T32-GM008799) at the University of California, Davis. Tanya Garcia-Nolan and Chrisoula Toupadakis Skouritakis of the Veterinary Orthopedic Research Laboratory at the University of California, Davis assisted in obtaining the μCT data.

REFERENCES

1. Castano-Izquierdo H, Alvarez-Barreto J, van den Dolder J, Jansen JA, Mikos AG, Sikavitsas VI. Pre-culture period of mesenchymal stem cells in osteogenic media influences their in vivo bone forming potential. Journal of biomedical materials research Part A. 2007; 82:129–138. [PubMed: 17269144]
2. Ye X, Yin X, Yang D, Tan J, Liu G. Ectopic bone regeneration by human bone marrow mononucleated cells, undifferentiated and osteogenically differentiated bone marrow mesenchymal stem cells in beta-tricalcium phosphate scaffolds. Tissue engineering Part C Methods. 2012; 18:545–556. [PubMed: 22250840]
3. Peters A, Toben D, Lienau J, Schell H, Bail HJ, Matziolis G, et al. Locally applied osteogenic predifferentiated progenitor cells are more effective than undifferentiated mesenchymal stem cells in the treatment of delayed bone healing. Tissue engineering Part A. 2009; 15:2947–2954. [PubMed: 19302033]
4. Mankani MH, Kuznetsov SA, Robey PG. Formation of hematopoietic territories and bone by transplanted human bone marrow stromal cells requires a critical cell density. Experimental Hematology. 2007; 35:995–1004. [PubMed: 17960668]
5. Peng H, Wright V, Usas A, Gearhart B, Shen HC, Cummins J, et al. Synergistic enhancement of bone formation and healing by stem cell-expressed VEGF and bone morphogenetic protein-4. The Journal of clinical investigation. 2002; 110:751–759. [PubMed: 12235106]

6. Banfi A, Muraglia A, Dozin B, Mastrogiacomo M, Cancedda R, Quarto R. Proliferation kinetics and differentiation potential of ex vivo expanded human bone marrow stromal cells: Implications for their use in cell therapy. Experimental hematology. 2000; 28:707–715. [PubMed: 10880757]
7. Bertolo A, Mehr M, Janner-Jametti T, Graumann U, Aebli N, Baur M, et al. An in vitro expansion score for tissue-engineering applications with human bone marrow-derived mesenchymal stem cells. Journal of tissue engineering and regenerative medicine. 2013
8. Digirolamo CM, Stokes D, Colter D, Phinney DG, Class R, Prockop DJ. Propagation and senescence of human marrow stromal cells in culture: a simple colony-forming assay identifies samples with the greatest potential to propagate and differentiate. British journal of haematology. 1999; 107:275–281. [PubMed: 10583212]
9. Muraglia A, Cancedda R, Quarto R. Clonal mesenchymal progenitors from human bone marrow differentiate in vitro according to a hierarchical model. Journal of cell science. 2000; 113(Pt 7): 1161–1166. [PubMed: 10704367]
10. Hoch AI, Leach JK. Concise review: optimizing expansion of bone marrow mesenchymal stem/stromal cells for clinical applications. Stem cells translational medicine. 2014; 3:643–652. [PubMed: 24682286]
11. Hoch AI, Binder BY, Genetos DC, Leach JK. Differentiation-dependent secretion of proangiogenic factors by mesenchymal stem cells. PLoS One. 2012; 7:e35579. [PubMed: 22536411]
12. Mayer H, Bertram H, Lindenmaier W, Korff T, Weber H, Weich H. Vascular endothelial growth factor (VEGF-A) expression in human mesenchymal stem cells: Autocrine and paracrine role on osteoblastic and endothelial differentiation. Journal of cellular biochemistry. 2005; 95:827–839. [PubMed: 15838884]
13. Jaiswal N, Haynesworth SE, Caplan AI, Bruder SP. Osteogenic differentiation of purified, culture-expanded human mesenchymal stem cells in vitro. Journal of cellular biochemistry. 1997; 64:295–312. [PubMed: 9027589]
14. Song L, Tuan RS. Transdifferentiation potential of human mesenchymal stem cells derived from bone marrow. FASEB journal. 2004; 18:980–982. [PubMed: 15084518]
15. Petrie TA, Raynor JE, Dumbauld DW, Lee TT, Jagtap S, Templeman KL, et al. Multivalent integrin-specific ligands enhance tissue healing and biomaterial integration. Science translational medicine. 2010; 2:45ra60.
16. Badylak SF, Freytes DO, Gilbert TW. Extracellular matrix as a biological scaffold material: Structure and function. Acta Biomateralia. 2009; 5:1–13.
17. Decaris ML, Mojadedi A, Bhat A, Leach JK. Transferable cell-secreted extracellular matrices enhance osteogenic differentiation. Acta Biomateralia. 2012; 8:744–752.
18. Decaris ML, Binder BY, Soicher MA, Bhat A, Leach JK. Cell-derived matrix coatings for polymeric scaffolds. Tissue engineering Part A. 2012; 18:2148–2157. [PubMed: 22651377]
19. Bhat A, Hoch AI, Decaris ML, Leach JK. Alginate hydrogels containing cell-interactive beads for bone formation. FASEB journal. 2013; 27:4844–4852. [PubMed: 24005905]
20. Decaris ML, Leach JK. Design of experiments approach to engineer cell-secreted matrices for directing osteogenic differentiation. Ann Biomed Eng. 2011; 39:1174–1185. [PubMed: 21120695]
21. He J, Decaris ML, Leach JK. Bioceramic-mediated trophic factor secretion by mesenchymal stem cells enhances in vitro endothelial cell persistence and in vivo angiogenesis. Tissue engineering Part A. 2012; 18:1520–1528. [PubMed: 22546052]
22. Li L, Chen Z, Zhang L, Xing Y, Kang K. A cone-beam tomography system with a reduced size planar detector: a backprojection-filtration reconstruction algorithm as well as numerical and practical experiments. Applied radiation and isotopes. 2007; 65:1041–1047. [PubMed: 17651975]
23. Aubin JE, Liu F, Malaval L, Gupta AK. Osteoblast and chondroblast differentiation. Bone. 1995; 17:S77–S83.
24. Aubin JE. Bone stem cells. Journal of cellular biochemistry. 1998:73–82. [PubMed: 9893258]
25. Schellenberg A, Hemeda H, Wagner W. Tracking of replicative senescence in mesenchymal stem cells by colony-forming unit frequency. Methods in molecular biology. 2013; 976:143–154. [PubMed: 23400440]

26. Russell KC, Phinney DG, Lacey MR, Barrilleaux BL, Meyertholen KE, O'Connor KC. In vitro high-capacity assay to quantify the clonal heterogeneity in trilineage potential of mesenchymal stem cells reveals a complex hierarchy of lineage commitment. Stem Cells. 2010; 28:788–798. [PubMed: 20127798]
27. Braccini A, Wendt D, Farhadi J, Schaeren S, Heberer M, Martin I. The osteogenicity of implanted engineered bone constructs is related to the density of clonogenic bone marrow stromal cells. Journal of tissue engineering and regenerative medicine. 2007; 1:60–65. [PubMed: 18038393]
28. Dennis JE, Haynesworth SE, Young RG, Caplan AI. Osteogenesis in marrow-derived mesenchymal cell porous ceramic composites transplanted subcutaneously: effect of fibronectin and laminin on cell retention and rate of osteogenic expression. Cell Transplantation. 1992; 1:23–32. [PubMed: 1344289]
29. Khatiwala CB, Kim PD, Peyton SR, Putnam AJ. ECM compliance regulates osteogenesis by influencing MAPK signaling downstream of RhoA and ROCK. Journal of bone and mineral research. 2009; 24:886–898. [PubMed: 19113908]
30. Ogura N, Kawada M, Chang WJ, Zhang Q, Lee SY, Kondoh T, et al. Differentiation of the human mesenchymal stem cells derived from bone marrow and enhancement of cell attachment by fibronectin. Journal of oral science. 2004; 46:207–213. [PubMed: 15901064]
31. McBeath R, Pirone DM, Nelson CM, Bhadriraju K, Chen CS. Cell shape, cytoskeletal tension, and RhoA regulate stem cell lineage commitment. Developmental cell. 2004; 6:483–495. [PubMed: 15068789]
32. He J, Genetos DC, Leach JK. Osteogenesis and trophic factor secretion are influenced by the composition of hydroxyapatite/poly(lactide-co-glycolide) composite scaffolds. Tissue Engineering Part A. 2010; 16:127–137. [PubMed: 19642853]
33. Kaigler D, Wang Z, Horger K, Mooney DJ, Krebsbach PH. VEGF scaffolds enhance angiogenesis and bone regeneration in irradiated osseous defects. Journal of bone and mineral research. 2006; 21:735–744. [PubMed: 16734388]
34. Leu A, Stieger SM, Dayton P, Ferrara KW, Leach JK. Angiogenic response to bioactive glass promotes bone healing in an irradiated calvarial defect. Tissue engineering Part A. 2009; 15:877–885. [PubMed: 18795867]
35. Blau HM, Brazelton TR, Weimann JM. The evolving concept of a stem cell: entity or function? Cell. 2001; 105:829–841. [PubMed: 11439179]
36. Colter DC, Class R, DiGirolamo CM, Prockop DJ. Rapid expansion of recycling stem cells in cultures of plastic-adherent cells from human bone marrow. Proceedings of the National Academy of Sciences of the United States of America. 2000; 97:3213–3218. [PubMed: 10725391]
37. Sekiya I, Larson BL, Smith JR, Pochampally R, Cui JG, Prockop DJ. Expansion of human adult stem cells from bone marrow stroma: Conditions that maximize the yields of early progenitors and evaluate their quality. Stem cells. 2002; 20:530–541. [PubMed: 12456961]
38. Beresford JN, Bennett JH, Devlin C, Leboy PS, Owen ME. Evidence for an inverse relationship between the differentiation of adipocytic and osteogenic cells in rat marrow stromal cell-cultures. Journal of cell science. 1992; 102:341–351. [PubMed: 1400636]
39. Binder BY, Genetos DC, Leach JK. Lysophosphatidic acid protects human mesenchymal stromal cells from differentiation-dependent vulnerability to apoptosis. Tissue engineering Part A. 2014; 20:1156–1164. [PubMed: 24131310]
40. Rowley JA, Madlambayan G, Mooney DJ. Alginate hydrogels as synthetic extracellular matrix materials. Biomaterials. 1999; 20:45–53. [PubMed: 9916770]
41. Engler AJ, Sen S, Sweeney HL, Discher DE. Matrix elasticity directs stem cell lineage specification. Cell. 2006; 126:677–689. [PubMed: 16923388]

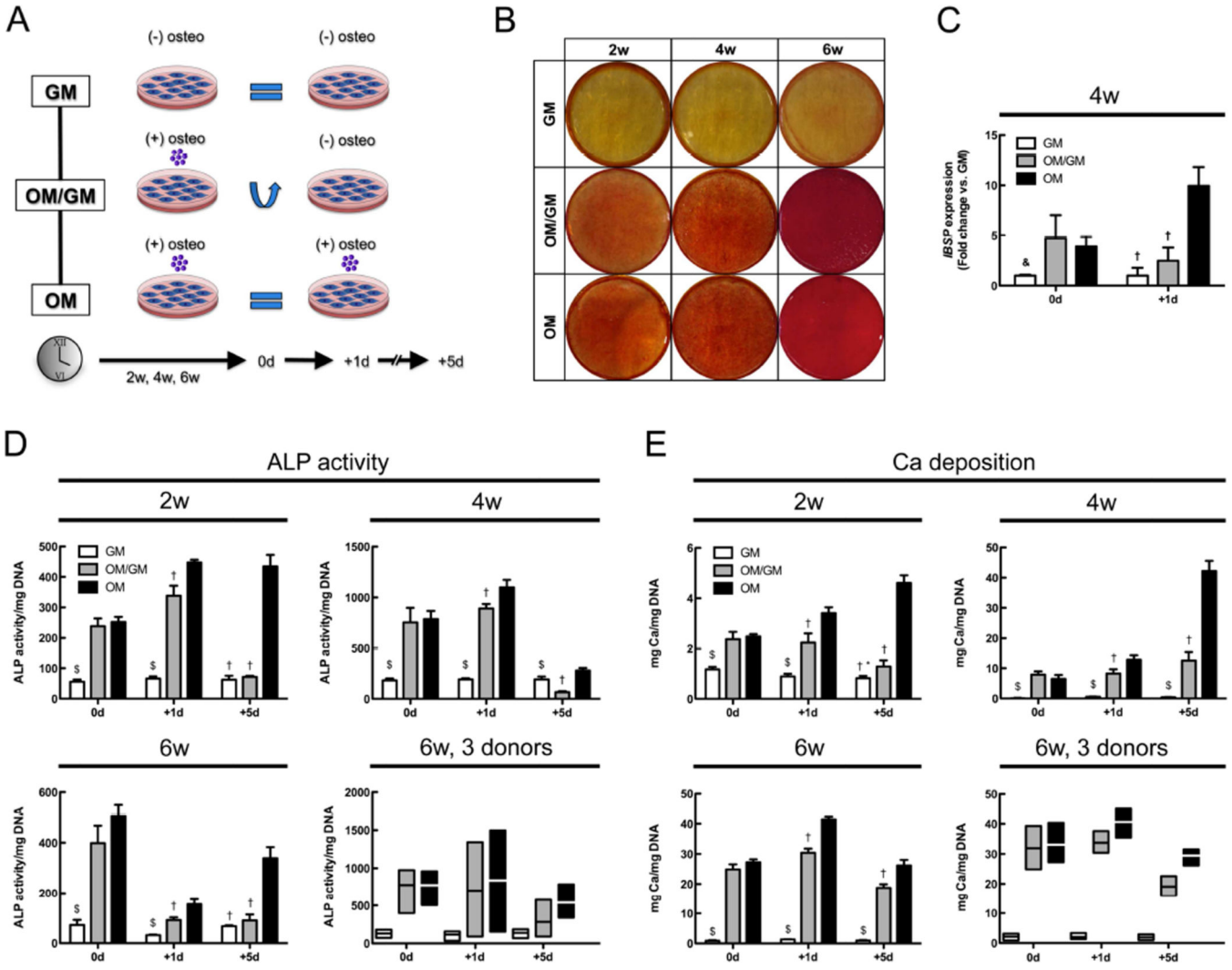

FIGURE 1. Osteogenic markers rapidly regress upon the withdrawal of the osteogenic cocktail

A) After 2, 4, and 6 weeks, osteogenic supplements were removed from one group of osteogenically differentiated MSCs (OM/GM). Osteogenic markers were assessed at 0d, +1d, and +5d. B) Representative Alizarin Red S staining of mineralized matrix after 2, 4, and 6 week culture at baseline (0d). C) Bone sialoprotein (*IBSP)* expression after 4 weeks. D) Normalized alkaline phosphatase (ALP) activity and E) normalized calcium deposition for 2, 4, and 6 weeks of osteogenic differentiation. Chart values represent mean ± SD for n = 3–4; $^{\$}p<0.001$ vs. OM/GM and OM, $^{\dagger}p<0.001$ vs. OM, $^{*}p<0.05$ vs. OM/GM all within same day. Chart values for 3 donors span data points and the line signifies the mean.

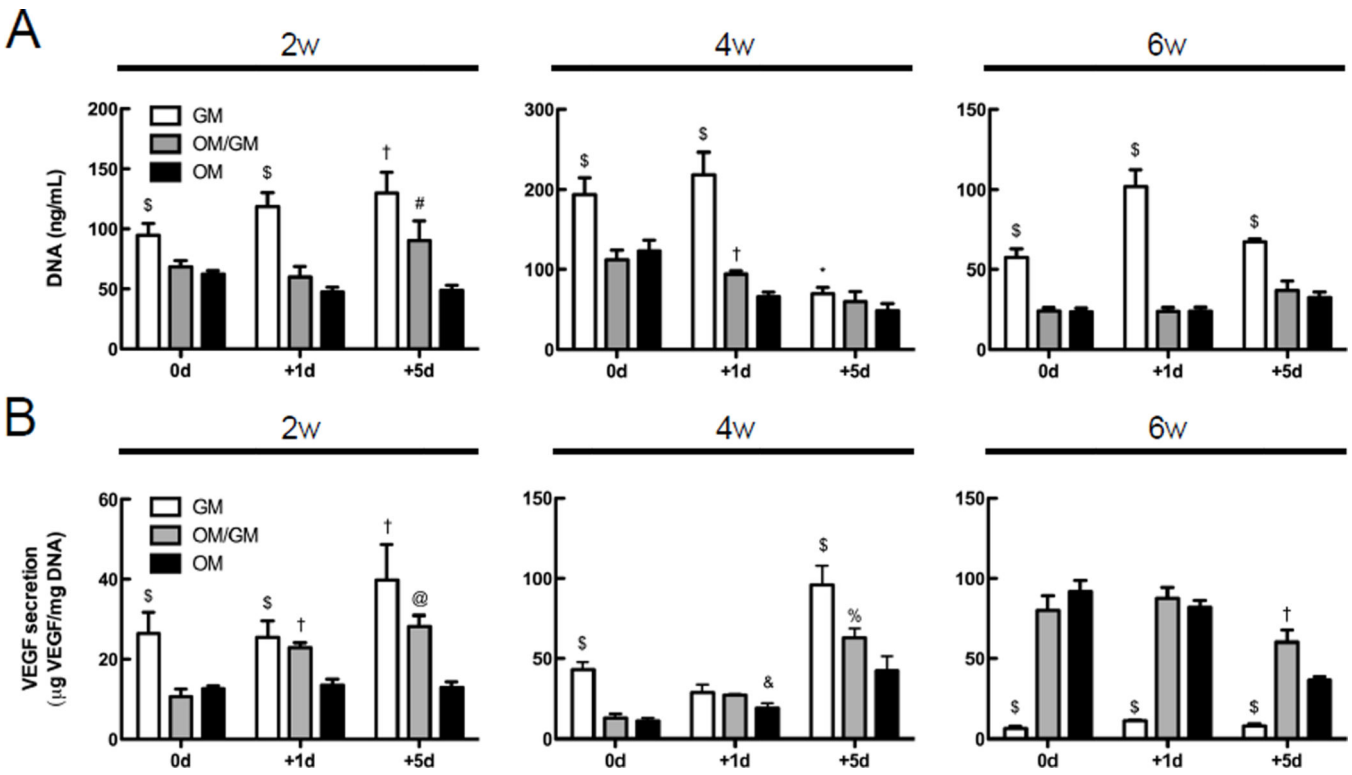

FIGURE 2. MSC proliferation and VEGF secretion and are impaired during osteogenic differentiation

A) DNA concentration and B) normalized vascular endothelial growth factor (VEGF) secretion for MSCs cultured for 2, 4, and 6 weeks. Chart values represent mean ± SD for n = 3–4, $^{\$}p<0.001$ vs. OM/GM and OM, $^{\dagger}p<0.001$ vs. OM, $p<0.01$ vs. OM, $^{\&}p<0.01$ vs. OM/GM and GM, $^{\%}p<0.05$ vs. OM, $^{\#}p<0.01$ vs. GM and OM, $^{*}p<0.05$ vs. OM all within same day.

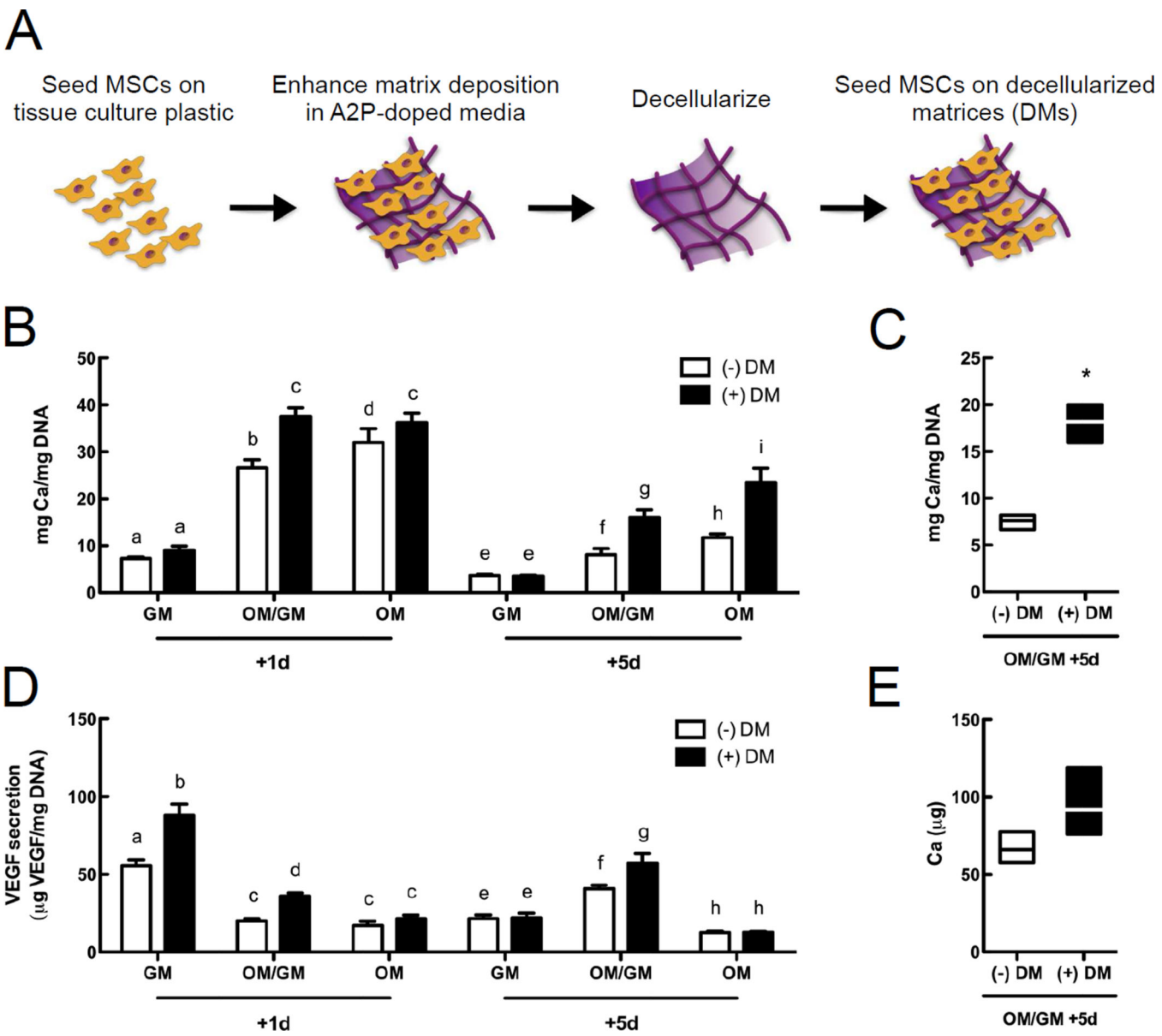

FIGURE 3. Decellularized matrices (DMs) enhance calcium deposition and VEGF secretion by differentiated MSCs in the absence of the osteogenic cocktail

A) MSCs secrete extracellular matrix, which is subsequently decellularized and can be stored and transferred. B) Normalized calcium deposition by MSCs cultured in growth media and osteogenic media for 2 weeks and seeded on tissue culture plastic ((−) DM) or decellularized matrices ((+) DM). C) Normalized calcium across three MSC donors. D) Normalized vascular endothelial growth factor (VEGF) secretion by MSCs. E) Total calcium secreted by MSCs from three biological donors. Chart values represent mean ± SD for n = 3–4; bars not connected by the same letter are significantly different ($p<0.05$) all within same day; *$p<0.05$ vs. (−) DM. Chart values for 3 donors span data points and the line signifies the mean.

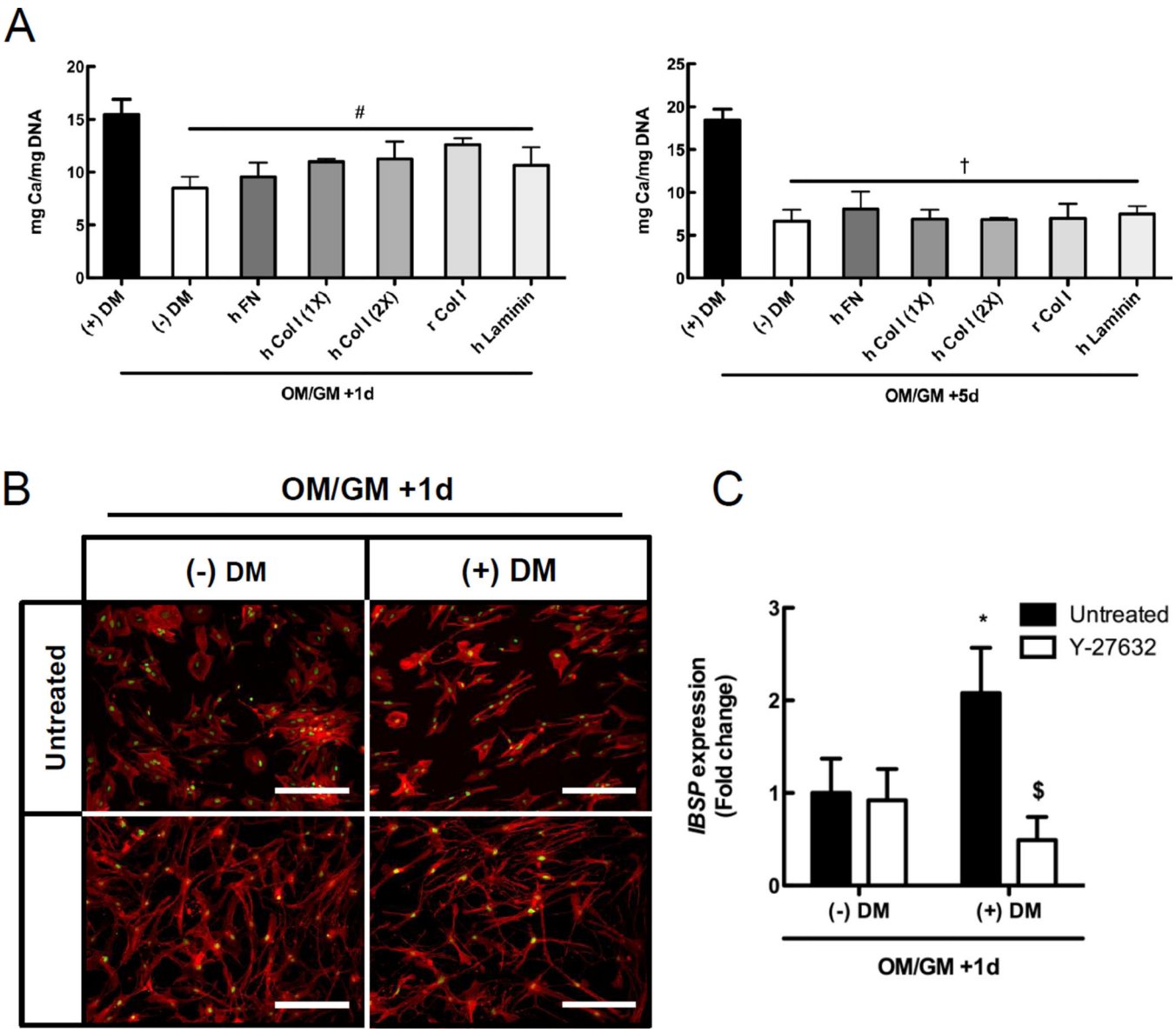

FIGURE 4. Decellularized matrices (DMs) preserve calcium deposition compared to individual matrix constituents and function partially through ROCK II

A) Normalized calcium deposition by MSCs cultured in osteogenic media for 2 weeks and seeded on tissue culture plastic ((−) DM), decellularized matrices ((+) DM), human fibronectin (h FN), human collagen type I (h Col I (1×) and h Col I (2×), denoting two concentrations of the protein), rat tail collagen type I (r Col I), and human laminin-α4 (h Laminin). B) F-actin staining using rhodamine phalloidin (*red*) and SYTOX® Green nuclear stain (*green*) of untreated osteogenically differentiated MSCs and osteogenically differentiated MSCs exposed to 10 μM Y-27632 for 24 hours. Scale bars represent 200 μm. C) Bone sialoprotein (*IBSP)* expression of untreated osteogenically differentiated MSCs and osteogenically differentiated MSCs exposed to Y-27632 for 24h. Chart values represent mean ± SD for n = 3–4; $^{\#}p<0.05$ vs. (+) DM, $^{\dagger}p<0.001$ vs. (+) DM, $^{*}p<0.01$ vs. untreated (−) DM, $^{\$}p<0.01$ vs. untreated (+) DM.

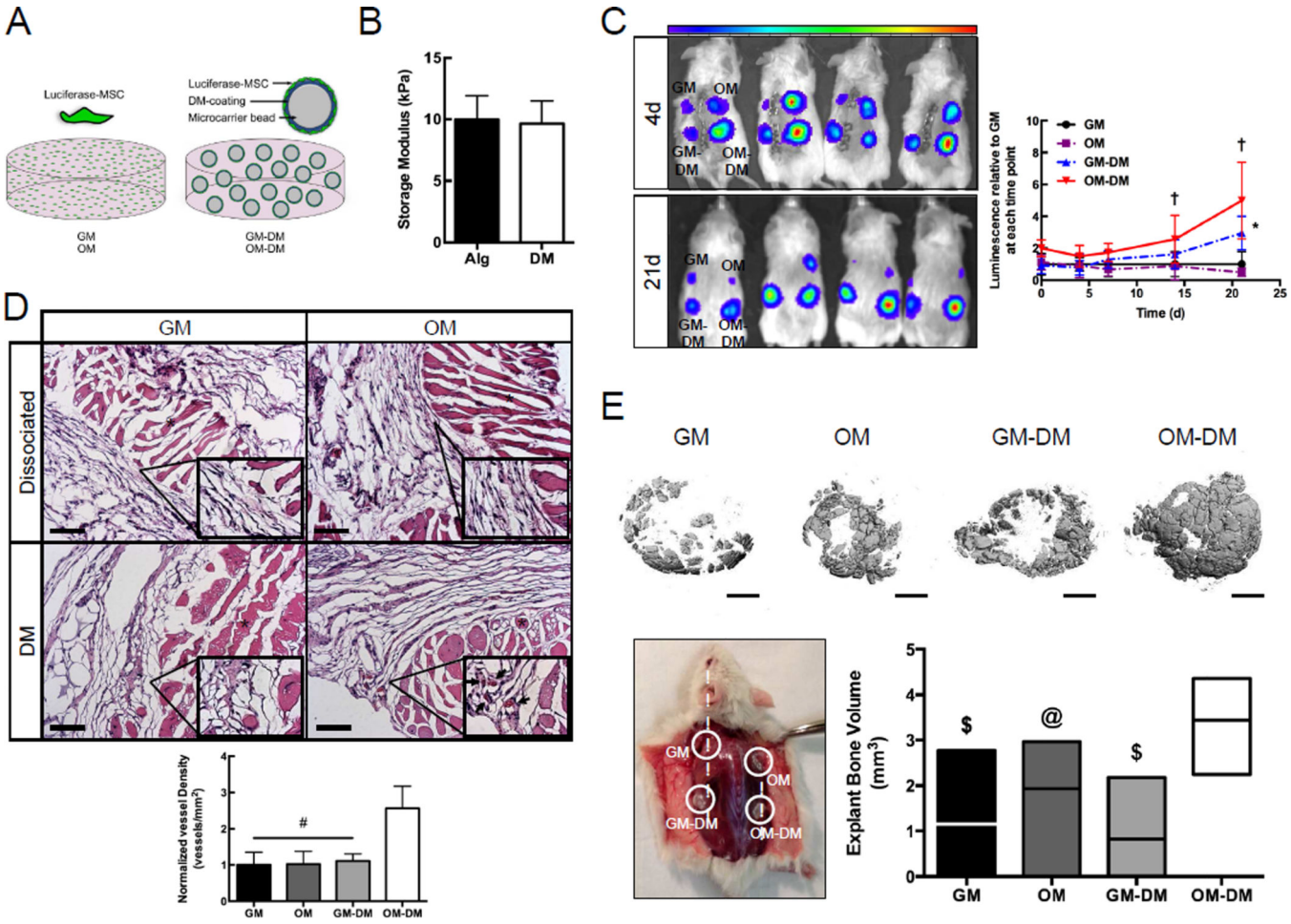

FIGURE 5. Osteogenically induced MSCs delivered with DMs exhibit increased cell persistence, vessel density, and bone formation in an ectopic tissue site

A) Luciferase-MSCs are deployed as dissociated cells or adhered to DM-coated microcarrier beads and embedded within an alginate hydrogel. B) Storage modulus of MSC-loaded alginate hydrogels (Alg) and hydrogels containing DM-coated beads (DM). C) Luminescence from low (blue) to high (red) at 4 days and 21 days. Top left: GM. Top right: OM. Bottom left: GM-DM. Bottom right: OM-DM. D) After 2 week ectopic implantation, OM-DM exhibited 3-fold greater vessel density in H&E stained cross-sections: 10× view, 40× insets, scale bars represent 100 μm. Asterisks indicate the hydrogel and arrows denote blood vessels. E) After 8 week ectopic implantation, OM-DM demonstrated significantly increased explant bone volume (mm^3) compared to other groups. Scale bars represent 1 mm. Chart values represent mean ± SD (n ≥ 6); $^{\dagger}p<0.05$ OM-DM vs. all groups at 14d and 21d, $^{*}p<0.05$ GM-DM vs. GM and OM at 21d, $^{\#}p<0.01$ vs. OM-DM, $^{\$}p<0.01$ vs. OM-DM, $p<0.05$ vs. OM-DM.